Geminate Recombination of Diatomic Ligands CO, O_2, and NO with Myoglobin†

Kevin N. Walda,‡ X. Y. Liu,‡ Vijay S. Sharma,§ and Douglas Magde*,‡

Department of Chemistry 0314 and Department of Medicine 0652, University of California at San Diego, 9500 Gilman Drive, La Jolla, California 92093

Received July 9, 1993; Revised Manuscript Received November 3, 1993®

ABSTRACT: The kinetics of geminate recombination of horse heart myoglobin with the diatomic ligands carbon monoxide, dioxygen, and nitric oxide have been reexamined. The new measurements are distinguished from previous studies by (1) consideration of the complete time range longer than 1 ps, (2) inclusion of the effect of temperature changes near ambient, (3) attention to the relation between recombination kinetics and the yield of dissociated partners on the millisecond time scale, and (4) use of singular value decomposition in the analysis. These picosecond results, together with earlier nanosecond data, for O_2 prove that models incorporating one, two, or even three discrete intermediates are not sufficient to account for all features of geminate recombination kinetics. Instead, a continuous evolution of the geminate pair distribution is preferred.

When light impinges on hemoglobin (Hb) or myoglobin (Mb) complexed with a ligand, L, photolysis of the coordinate bond may occur with an external quantum efficiency, Q, measured at microsecond or longer times, that varies widely with L (Antonini & Brunori, 1971). In 1979 it was recognized that those geminate partners remain in the protein for long times, e.g., hundreds of nanoseconds even at ambient conditions, in at least some cases (Alpert et al., 1979; Duddell et al., 1979). It later became clear that a wide variety of ligands remains in the protein, either Mb and Hb, for these long times (Henry et al., 1983; Gibson et al., 1986; Jongeward et al., 1988). The minimum model for binding is, therefore,

$$\underset{A}{[MbL]} \overset{k_1}{\underset{k_{-1}}{\rightleftharpoons}} \underset{B}{[Mb|L]} \overset{k_2}{\underset{k_{-2}}{\rightleftharpoons}} \underset{C}{[Mb + L]} \qquad (1)$$

where k_1 characterizes thermal bond dissociation, k_{-1} characterizes concentration-independent bond formation from the geminate pair, k_2 characterizes ligand escape from the protein, and k_{-2} is a concentration-dependent, bimolecular rate constant.

A decade ago, Agmon and Hopfield (AH) (1983) considered the influence of a surrounding protein matrix on reactivity at the binding site. They distinguished a reaction coordinate, which measures the progress of the ligand toward the binding site and is meant to be the same concept commonly used in mechanistic chemistry, from a second coordinate that represents, in some way, all of the influence of the surrounding protein and is taken to be orthogonal to the reaction coordinate. This orthogonal coordinate exerts its influence as a parameter that controls the shape of the reaction coordinate and determines, in particular, the height and location of any barrier along the reaction coordinate. AH suggested two measurable consequences of their model: at low temperatures, especially in a rigid, glass matrix, the protein should be frozen into one of a large set of alternative conformations, each of which is characterized by different reaction kinetics. Presumably, members of this ensemble also exhibit different spectra, although the differences might not always be measurable in practical experiments. The members of the ensemble interconvert very slowly or not at all.

In contrast, at ambient temperatures in fluid solution, the protein conformations will interconvert over a wide variety of time scales. At thermal equilibrium, there will be a distribution of conformations present in the ensemble. If a perturbation is applied to the system, the distribution existing before the perturbation may not be the "proper" distribution after the perturbation. The ensemble will relax toward the new distribution. One such perturbation is ligand dissociation by photolysis. The relaxed ensemble of conformations is likely to be different for the liganded and unliganded states. We might expect that the spectral properties will evolve over time subsequent to ligand dissociation. Similarly, the rate of recombination, k_{-1}, would be expected to vary in a continuous fashion over time as the distribution of states within the ensemble evolves. We cite AH because it is a good starting point for the issues we address and to acknowledge their influence on our ideas (Campbell, 1985). It is important to point out that AH were motivated by a decade of low-temperature experiments by Frauenfelder and his collaborators at the University of Illinois (Austin et al., 1975; Alberding et al., 1978), who showed that a heterogeneous population exists at low temperature. They have continued to refine their model (Ansari et al., 1987). The Illinois group certainly contemplated protein motion before AH (Beece et al., 1980). They were consistent in stressing that nonexponential rebinding should persist at intermediate (but still subambient) temperatures. However, at one time they seemed convinced that at ambient conditions geminate recombination kinetics might simplify to become a simple exponential, at least in Mb, if not necessarily in tetrameric Hb (Ansari et al., 1986). (Hemoglobin has a history of its own; we want to concentrate here on the simpler Mb.)

The specific contribution of AH was a particular theoretical treatment in which the protein conformation evolves diffusively and obeys a Smoluchowski function. The same general approach has been used by other theorists (Berlin et al., 1992). Recently, Agmon (1992) further developed his approach and discussed its theoretical development over the decade. Our interest here is only the general issue: We ask the experimental

† This work supported in part by NSF Grants CHE-8715561 and CHE-9114613. K.N.W. was an NIH Predoctoral Trainee.

* Author to whom correspondence should be addressed.
‡ Department of Chemistry.
§ Department of Medicine.

® Abstract published in *Advance ACS Abstracts,* January 15, 1994.

0006-2960/94/0433-2198$04.50/0

question of whether the coupling between the reaction coordinate and the matrix coordinate is such that the experimentally observed rebinding rate constant near room temperature evolves in a smooth and continuous fashion or exhibits abrupt transitions between states with rather different kinetic properties, so that only two or three discrete regimes are apparent in measurements. Our measurements do not address the following question: How much heterogeneity exists at any particular time after photolysis, that is, what is the variance in the distribution of conformations as a function of time? Champion and co-workers have treated this recently and cited earlier work by others (Champion, 1992; Tian et al., 1992). Since they concentrate on CO which, if not atrypical is at least a limiting case in that it exhibits the slowest recombination rate of all ligands, it would be premature to speculate on the relation to the results here.

If the AH model is useful, there should be fast recombination observable in picosecond experiments. Indeed, picosecond observations of recombination preceded recognition of the nanosecond process (Nöe et al., 1978; Greene et al., 1978). These were treated in isolation, without explicit concern for the entire time range. A systematic study of picosecond geminate pair behavior by the ENSTA group (Laboratorie d'Optique Appliqueé, Ecole Polytechnique–ENSTA) started in 1983 (Martin et al., 1983) and continues (Petrich et al., 1988) to the present, with a very pertinent study of NO binding (Petrich et al., 1991).

When we began an exploration of picosecond geminate recombination in a series of proteins and model hemes complexed to isocyanides and other ligands (Jongeward et al., 1988), we expected to find simple exponentials on a wide variety of different time scales at room temperature. Instead, we found that reaction rate constants clustered into two groups: characteristic times of much less than 50 ps or much longer than 10 ns. What varied was the amount of recombination in each ligand. Very little seemed to happen at intermediate times, and most ligands we studied showed both characteristic times. We proposed that some crucial conformational change in either the protein or the relation of the ligand to the surrounding protein, probably both, took place in about 10–20 ps. This could be accommodated by the AH (or any similar) interpretation, but it was an interesting case. It was just a two-intermediate, sequential reaction. We were aware that the intermediate time scale, spanning 2 orders of magnitude, was difficult to measure. However, at least for the isocyanides, we had accounted for all of the photolysis, and there was not much amplitude available to react at 1–10 ns.

The situation with diatomic ligands, however, which are more important biologically, was not as clear. Carbon monoxide recombined with so little Mb at any time that it would be impossible to resolve multiple phases. Nitric oxide recombined so efficiently at picosecond times that it was difficult to "follow" the recombination to longer times. Dioxygen was the most mysterious. Even though we resolved recombination on both time scales, there was "missing amplitude". There were, moreover, contradictions in the published data. We have now reexamined the diatomic ligands. We conclude that recombination does not occur with a single characteristic rate or even with two distinguishable exponential processes. Recombination occurs on all time scales and may best be discussed with some model that invokes the general ideas we learned from AH. The larger ligands, like isocyanides, presumably distort the protein pocket (Sommer et al., 1985), so that conformational changes and reorientation of the ligand take place with a more abrupt "switch" from a fast-reacting to a slow-reacting form. Presumably, the slow-reacting form faces a significant barrier that it must cross to regenerate the fast-reacting form—just as we proposed originally. However, the smaller diatomics do not admit of such a two-state approximation. Rather, we need a continuously evolving distribution of geminate pair configurations and protein conformations, each of which can be characterized by its own characteristic recombination rate.

While slow progress has been made in characterizing the geminate recombination kinetics, other experiments have revealed that a variety of relaxation processes probably do occur in the proteins on all time scales, from subpicosecond to microsecond (and longer for quaternary structural changes) even at ambient conditions. It is not possible yet to relate these to the AH "perpendicular coordinate" in any convincing manner, but they are suggestive. Time-resolved Raman scattering proves that the major relaxation in the iron movement relative to the porphyrin takes place within picoseconds (Findsen et al., 1985), and probably within a few hundred femtoseconds (Petrich & Martin, 1989), although other transients observed in Raman spectra evolve over the entire time scale of geminate recombination (Scott & Friedman, 1984; Dasgupta et al., 1985; Schneebeck et al., 1993). Time-resolved circular dichroism studies, which may be monitoring large-scale secondary or tertiary changes in the protein, reveal a 300-ps relaxation, which is an interesting time scale (Xie & Simon, 1990). Thermal phase gratings suggest both picosecond and nanosecond relaxations (Genberg et al., 1987). Detailed analysis of time-resolved visible absorption spectra using singular value decomposition revealed evidence for tertiary relaxation at times near 50 ns and 1 μs in Hb (Murray et al., 1988). Although similar features proved difficult to resolve in Mb, recent experiments seem to have found them (Lambright et al., 1991). At very low temperatures, where large conformational changes will be much slower, quite extensive data are available (Young et al., 1991). Only a portion has been integrated into the understanding of processes at ambient temperatures, but they suggest ample complexity to account for continuously evolving reaction rate constants. Computer simulations are consistent with the thermal accessibility of multiple states (Elber & Karplus, 1987; Steinbach et al., 1991), but it is still difficult to extend molecular dynamics calculations to long times with high precision.

EXPERIMENTAL PROCEDURES

Laser Apparatus. The laser used for picosecond measurements is a colliding-pulse mode-locked ring dye laser (CPM) followed by a four-stage dye amplifier running at 10 Hz. A Spectra-Physics Model 2020 CW argon ion laser operating "all lines" pumps the CPM. The gain medium is rhodamine 590 chloride in ethylene glycol. The vertical dye jet is oriented at Brewster's angle to the horizontally polarized pump. Passive mode-locking is achieved by DODC iodide in ethylene glycol flowing through a thin jet. Both dye solutions are cooled to 18 °C.

The two counterpropagating pulses strike the output coupler at different angles, producing two output beams. One output train is sent down the amplifier chain. The other is used for diagnostic purposes and to trigger the amplifier. Part of each diagnostic pulse is reflected from a diffraction grating to monitor the pulse spectrum. Another portion goes to an autocorrelator, whose output is displayed continuously. The last part is focused onto a photodiode. After electronic amplification, the photodiode signal is used to monitor millisecond fluctuations in the ring. A second output from

the amplifier is used to drive an electronic circuit that synchronizes the operation of the amplifier.

The dye amplifier consists of four gain stages separated by three saturable absorber jets. The amplifier is optically pumped by the second harmonic (532 nm) of a Quanta-Ray Model DCR-2A Q-switched Nd:YAG laser. A pair of prisms partially compensates for the temporal dispersion that the pulse undergoes as it propagates down the amplifier chain. We use rhodamine 640 perchlorate in the first three stages and sulforhodamine in the fourth. The solvent is a 2% ammonyx/water solution. Jet streams of malachite green in ethylene glycol serve as saturable filters between stages in order to reduce amplified spontaneous emission (ASE).

After the last amplifier stage, each pulse has an energy of approximately 1 mJ, with 10% ASE and peak-to-peak fluctuations of 10%. This amplified beam is focused into a KDP crystal with a 200-mm focal length lens. The output from the KDP is 55–70 μJ of 314-nm light; this is used as the photolysis pulse. The 314-nm pulse is separated from the fundamental by a dichroic beam splitter, sent down a fixed delay line, and focused into the sample cell. The residual 628-nm light is sent down a variable delay line, which has a 5-cm hollow corner cube mounted on a motorized translation stage. The motor drive has a 15-cm range, allowing data to be acquired continuously in subpicosecond steps in the interval 0–1 ns. In addition, the motor stage is mounted on a track that is 1.5 m in length. Data can be collected under manual control out to 10 ns.

After the delay line, the 628-nm light is focused by a 50-mm focal length lens into a 10-mm cuvette containing water. Self-phase modulation generates a white light continuum. Typical energy in the blue is approximately 0.5 μJ per 100 nm. The continuum light is recollimated with a 50-mm focal length achromat. A colored glass filter selects a region of light to be used for probing the sample. A polarizer is used to give "magic angle" polarization between pump and probe beams. A portion of the continuum is focused onto a silicon photodiode and fed into a Stanford Research SR250 box car integrator, which monitors system performance and allows the normalization of transmission measurements. The pump and probe beams are combined collinearly with a UV-reflecting dichroic and focused by a quartz lens into the sample cell, which is positioned so that the probe beam is focused to a smaller diameter ($\sim$1 mm) than the pump beam ($\sim$2 mm), ensuring that the probe is sampling a region uniformly illuminated by the pump.

The sample cell is a recirculating flow cell with a total volume typically of 6 mL. For certain samples, which degraded under prolonged photolysis, large amounts ($\sim$50 mL) were prepared, flowed through the cell once, and discarded.

After passing through the sample cell, the probe beam is recollimated with a quartz lens and focused by a cylindrical lens onto the entrance slit of a spectrograph, which images the spectrum onto a Princeton Instruments Model IRY-700 intensified photodiode array run by an ST-120 controller interfaced to an "AT" class microcomputer. Software provided by Princeton Instruments is used to set up the controller and collect the data.

Data Acquisition and Processing. The experiments are of the pump/probe type. The 314-nm UV beam produces a transient population, and a probe beam interrogates that population at different times. We alternated pumped and unpumped transmittance measurements, using a computer-controlled mechanical shutter to block and unblock the pump beam. A "normalization" photodiode, mentioned above, monitors each continuum, even though it does not record each wavelength separately. Home-built electronics synchronize the blocking and unblocking of the pump beam with the movement of the delay line and control the step size, which can be set to $^1/_6$, $^1/_2$, or 1 ps. A typical data set consists of 5–10 scans of the delay line, with 20–40 pumped and unpumped pairs being collected at each delay position for each scan. The latter are averaged together, but the repetitive scans are processed separately to check for sample degradation. Each spectrum is reduced to 360 different wavelengths by discarding unintensified diodes and summing adjacent pairs of diodes. The compressed data consist of averaged intensity values for the pumped and the unpumped spectra at each of 360 wavelengths and a few hundred delay positions. These data are converted to delta absorbance values using

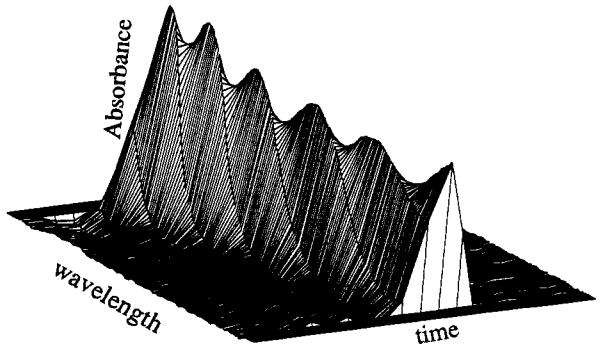

FIGURE 1: Two-photon absorption in toluene.

$$\Delta A = \log\left[\frac{(P-B)/N_P}{(U-B)/N_U}\right] \quad (2)$$

where P and U are the pumped and unpumped spectra, N_P and N_U are the normalization factors for each data point, and B is a background or dark current reading for the photodiode array. The ΔA files for different scans of the delay are inspected for drift and then averaged. If the transient absorbs more light than the unpumped species, ΔA will be positive. If the transient absorbs less light, ΔA will be negative; this is transient bleaching.

We discovered that toluene shows a two-photon absorption when pumped at 314 nm that is very easy to observe in the 375–500-nm region. We used this to determine the system response, as it involves no perturbation of the normal setup. Figure 1 shows a two-photon transient spectrum of toluene from 0 to 5 ps. From the singular value decomposition (SVD), we determine that there is 4.5 ps of temporal dispersion between extreme wavelengths in the probe pulse. To determine the system response, we examine the absorbance of a single wavelength versus time. The full-width at half-maximum (FWHM) is 2.5 ps. Deconvolution allows analysis to 1 ps or better.

Singular Value Decomposition. SVD has been used successfully by other groups to analyze microsecond and nanosecond transient data (Hofrichter et al., 1985; Lambright et al., 1991). This is the first use of SVD to analyze picosecond data that we are aware of. According to the SVD theorem, the $m \times n$ ΔA matrix can be written as the product of three matrices:

$$\Delta\mathbf{A} = \mathbf{U}\cdot\mathbf{S}\cdot\mathbf{V}^T \quad (3)$$

where ΔA is an $m \times n$ matrix consisting of absorbance changes at m wavelengths and n different time delays, U is an $m \times n$ matrix consisting of n orthonormal basis spectra, S is an $n \times n$ diagonal matrix containing the positive square roots of

the eigenvalues (singular values) of **A**, such that $S_{11} \geq S_{22} \cdots \geq 0$, and **V** is an $n \times n$ matrix whose columns (rows of $\mathbf{V}^T$) contain the time course amplitude for the corresponding basis spectra in matrix **U**. The singular values are a measure of the contribution of each basis spectrum to the data. Therefore, the first column of **U** multiplied by its singular value is the best single basis spectrum, which when multiplied by its time course amplitude, the first column of **V**, is the best one-component representation of the original transient spectra matrix $\Delta\mathbf{A}$. Columns 1 and 2 of **U** multiplied by their singular values and columns 1 and 2 of **V** are then the best two-component representation of $\Delta\mathbf{A}$, and so forth. The most useful information about the spectra is contained in the first few components, with the higher components representing noise.

A simple statistic for characterizing the significance of any column of **U** is the autocorrelation of order 1:

$$C_{U\ \mathrm{col}\ j} = \sum_{i=1}^{n} U_{ij} U_{i+1\,j} \qquad (4)$$

Typically, the autocorrelation value for a significant column of **U** should be greater than 0.5. A similar criterion exists for the columns of **V**. The differences between successive singular values of **S** also offer information as to the significance of the corresponding basis spectra. At first the differences will be large. Later singular values are smaller, nearly equal to their neighbors, and of little significance. All SVD calculations were performed on an "industry standard" 486 clone using 386-Matlab from Mathworks.

The SVD spectra do not necessarily correspond to the spectra of chemical species. In fact, if the chemical species have overlapping bands, the SVD spectra cannot all be spectra of chemical species, since the spectra in the basis set are orthogonal to each other. If all kinetic intermediates were members of a set with known spectra, it would be possible to calculate which linear combination of those intermediates best reproduced the SVD basis spectra. Unfortunately, for picosecond studies of myoglobin, we do not know the spectra of intermediates that might be present. We do not even know how many intermediates might occur. In fact, we must expect that the intermediates do not exist in thermodynamic equilibrium with well-defined spectra, but rather are nonequilibrium species that undergo vibrational relaxation with spectra that evolve continuously over time.

Sample Handling. A Lauda R-6 temperature bath was used to provide thermal regulation of the sample and the sample cell. The oxygen samples were kept under a constant positive pressure of oxygen. Nitrogen was used over the CO and NO samples. For each ligand, runs at two temperatures were performed on the same day. A large (~20 mL) sample was prepared and split in two, with one half being used for each temperature. A static spectrum was measured before and after each experiment. Any run that showed a change of more than a few percent was discarded.

Photolysis Quantum Yield. A Lumonics Model 861T excimer laser operating with an XeCl gas mixture pumps a dye oscillator–amplifier combination. Coumarin 540 dye produces a 4-ns pulse at a repetition rate of 1 Hz and a wavelength of 540 nm. In order to ensure uniform excitation of the sample, this optical pulse traverses a beam homogenizer, which splits the pulse into dozens of pieces by multiple reflections and then superimposes those pieces on the sample, exciting a 2 × 2 mm cross-section of the cuvette. The energy measured in the front of a sample cell is about 1 mJ, as measured by a Laser Precision Rj 7100 energy meter. This photolysis pulse is attenuated as required by glass neutral density filters.

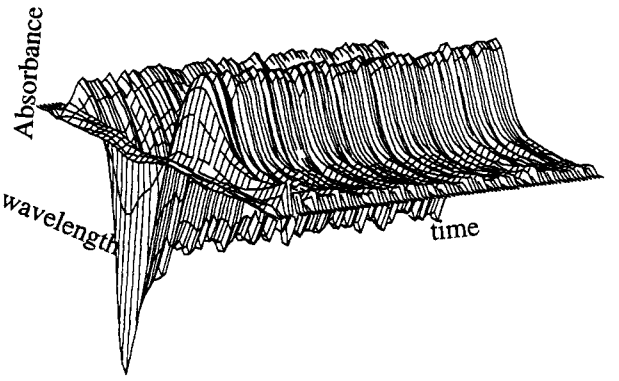

FIGURE 2: Corrected transient absorption spectra of MbO_2 at 12 °C, from 0 to 50 ps.

Continuous light from a highly stable tungsten halogen bulb monitors the sample absorbance over an area somewhat smaller than the region pumped. Small monochromators are located before and after the sample. The pump and probe beams are collinear. The transient absorption signal is detected by a photomultiplier, digitized and recorded by a Biomation Model 805 waveform recorder, and sent to a small microcomputer. The time resolution of the recordings used in the measurements reported is 1 μs/channel, and 2048 data points are collected for each curve. For each "run", 50 laser shots are averaged. Approximately 200 channels are recorded before the laser excitation. With this information, the record of transmittance is converted to a record of ΔA; the latter is fit to sums of exponentials using a nonlinear least-squares algorithm. All software was developed in-house.

The protein sample is contained in a 2-mm path length flow cell connected to a reservoir and recirculated by a gas-tight pump system. The flow rate is 2.5 mL/min. The sample is completely replaced between shots.

Sample Preparation. Horse heart myoglobin was purchased from Sigma and used with no further purification. The following procedure prepares approximately 1 mL of a 2000 μM myoglobin solution. Myoglobin (20 mg) is placed in a test tube and dissolved in a minimal amount of 0.1 M Bis-Tris ([bis(2-hydroxyethyl)amino]tris(hydroxymethyl)methane) buffer (pH 7.0). The sample is filtered through a syringe with some glass wool at the bottom. The solution is degassed, and a minimal amount of sodium dithionite is added to the Mb solution. The sample is passed anaerobically through a Sephadex G-25 column to remove the dithionite. The sample obtained in the above step is flushed with O_2 or CO to form either the oxy or carboxy derivative. For the preparation of the nitrosyl derivative, the MbO_2 derivative was deoxygenated for 1 h with nitrogen and then flushed with NO gas.

RESULTS

Myoglobin–O_2. Figure 2 shows myoglobin–oxygen transient spectra obtained at subambient temperature, 12 °C, with delay times from 0 to 50 ps. Although for clarity only the first 50 ps are shown, the SVD analysis was performed on the entire data set, which extends to 200 ps. The spectra displayed have been corrected for temporal dispersion, as measured using two-photon absorption of toluene. Table 1 gives the autocorrelation values for **U** and **V** along with the singular values of **S**. By commonly invoked criteria (autocorrelation values greater than 0.5), the first three components

Table 1: Results of the SVD Analysis of MbO_2

autocorrelation of U	autocorrelation of V	singular value of S
0.9950	0.9927	7.7616
0.9955	0.8045	0.6630
0.9959	0.5403	0.3349
0.9931	0.4383	0.2673
0.9658	0.0915	0.1871

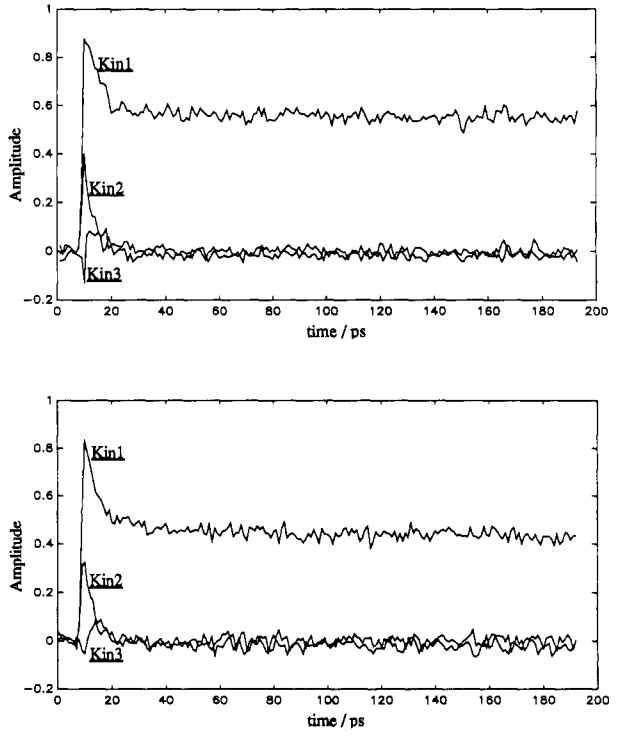

FIGURE 3: First three kinetic components obtained from the SVD analysis of the MbO_2 data obtained at 12 (top) and 34 °C (bottom).

are significant. However, there is no sharp division, suggestive of one or two distinct kinetic intermediates.

Figure 3 shows the time course of the first three kinetic components at 12 and 34 °C. Results at the two temperatures are essentially identical. Figure 4 shows the first two spectral components at the two temperatures. Again, there is no significant variation over this temperature range.

The first spectral component, spec1, closely corresponds to a deoxyMb minus oxyMb difference spectrum, as would be measured in a static experiment, although there is a small shift. We predominantly attribute the decay of this spectrum to geminate recombination. The second spectral component, spec2, is the first-order difference between the transient absorbance and spec1. It has some characteristics that have been observed before (Petrich et al., 1988; Jongeward et al., 1988), such as the red edge that extends from 450 nm out past 490 nm. We believe that this spectrum represents contributions from both electronically excited states and hot ground states. The third and higher components represent successively higher order difference spectra, corresponding to the difference between the measured absorbance and the weighted sum of all lower components. Each displays one additional node, or zero-crossing, in the spectrum (and also in the kinetic trace). We do not show them because they are certainly distorted both by the limited precision of our correction for the temporal dispersion in the probe beam and by random noise. There is no reason to think that the successive difference spectra should be distinct chemical species, even electronic or vibrational states. Instead, our preferred interpretation is that they

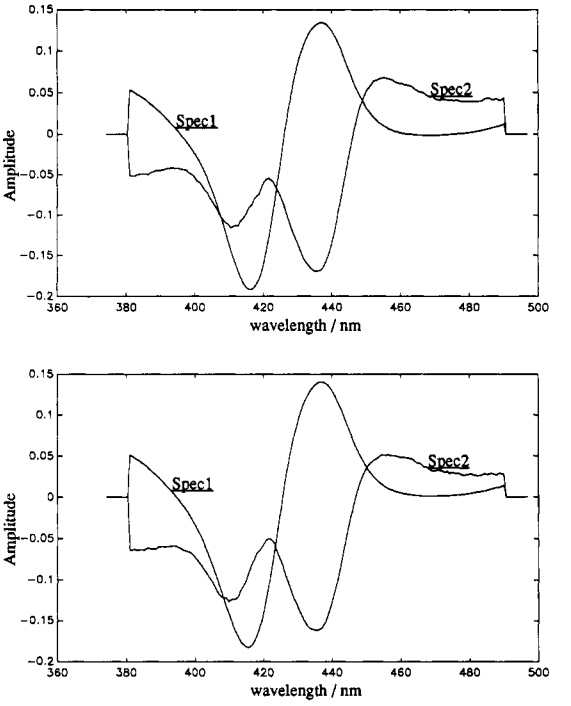

FIGURE 4: First two spectral components obtained from the SVD analysis of the MbO_2 data obtained at 12 (top) and 34 °C (bottom).

Table 2: Rate Constants for the SVD Analysis of MbO_2

sample (temp, °C)	k (s^{-1})	τ ($1/k$) (ps)	percent decay
Mb–O_2 (12)	$(1.54 \pm 0.5) \times 10^{11}$	6.5 ± 2	44 ± 5
Mb–O_2 (34)	$(1.56 \pm 0.5) \times 10^{11}$	6.4 ± 2	48 ± 5

characterize a transient difference spectrum that is shifting smoothly while it decays. Simulations that applied an identical SVD analysis to artificially constructed transient spectra shifting smoothly in time give results similar to those in Table 1 and associated figures.

We fit the kinetic components with single-exponential decays that have a base-line offset. Table 2 lists the rate constants, lifetime, and percent recovery, kin1, of Mb–O_2 at 12 and 34 °C. There is no difference. The higher components, whatever their assignment, are also virtually identical. These experiments show that the rate of geminate recombination of ground-state myoglobin to oxygen between 0 and 200 ps is not temperature-dependent near room temperature.

We previously reported the kinetics of geminate rebinding of oxygen with both horse heart and sperm whale Mb for times greater than 20 ns (Chatfield et al., 1990). We restate the pertinent observations briefly: nanosecond geminate rebinding of oxygen to horse heart myoglobin (HHMb) in 0.1 M Bis-Tris/0.1 M NaCl at 6, 16, and 25 °C exhibited multiexponential behavior, even though at 35 °C the data could be fit with a single exponential. We chose to fit the data at 6, 16, and 25 °C to double exponentials, although there was no a priori justification for doing so. We monitored the rebinding kinetics of O_2 to HHMb at 15.4 °C as a function of the probe wavelength. The amplitude ratios and rates derived from the biexponential fits at 430, 435, 440, and 445 nm were the same within experimental uncertainty, indicating that the multiexponential decays were not due to spectral shifts. We concluded that geminate recombination in horse heart Mb does display a limiting exponential behavior at long times, where it is most easily studied, but with sufficient resolution, deviations can be detected at early (<100 ns) times.

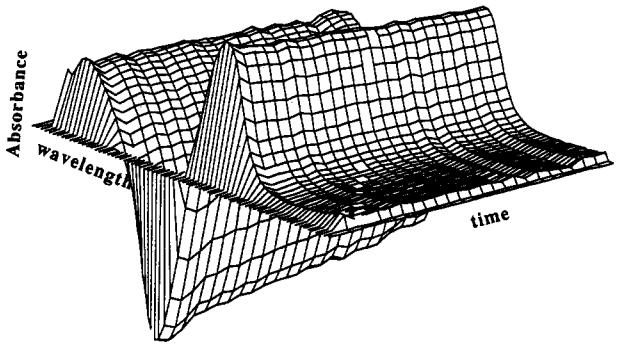

FIGURE 5: Transient absorbance for MbO_2 from 0 to 8 ns.

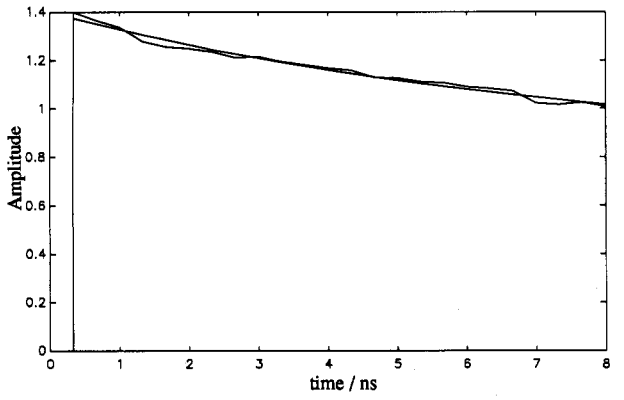

FIGURE 6: Single-exponential fit to the first kinetic component obtained from the SVD analysis of the 0–8-ns MbO_2 data.

A different Mb (sperm whale) and a second buffer system displayed kinetics that differ in detail but share the basic feature that, at subambient temperature and good enough experimental precision, a faster rebinding reveals itself. We suppose that the protein evolves toward some limiting conformation and that it reaches that limit more quickly at higher temperatures.

It was, therefore, essential in the present study to determine whether there was any recombination between that found with the picosecond apparatus (1.7×10^{11} s^{-1}) and that found with the nanosecond apparatus ($(1.7–3.7) \times 10^{7}$ s^{-1}). We used the CPM laser to look at the first 8 ns after photolysis. A serious challenge was ensuring that the probe beam did not change position with such large movements of the retroreflector. Visual examination was used to align the beam as well as possible, but an additional control was desired. We used horse heart MbCO as a reference, by assuming that it has negligible recombination.

Horse heart MbO_2 was measured in the flow cell at 25 °C. For each run, 200–300 spectra were collected at intervals of 333 ps. Figure 5 shows the raw transient data obtained for the $HHMbO_2$ sample from 0 to 8 ns after photolysis. To be consistent with the procedures used with the picosecond data, SVD analysis was performed on these data. Singular values dropped abruptly after the first component (5.75, 0.16, 0.11, 0.05). Only the first component had autocorrelation values for U and V that were greater than 0.5. Although it would be attractive to assign the minor components to spectral evolution associated with protein conformational changes near 1 ns, we cannot defend such an assignment with any great confidence. The first spectral component obtained from SVD analysis corresponds very closely to the static difference spectrum. Figure 6 shows the first kinetic component obtained from the SVD analysis, along with a single-exponential fit. The fraction recombining is 42%, and the lifetime is 8 ns. These numbers have larger than usual probable errors (on the order of 20%), since there is less than 1 half-life of data being fit. For that reason, it was also impossible to make a good measure of the effect of changing temperature. This recombination rate is much less than any rate observed at early picosecond times, but it is much greater than those observed at longer nanosecond times. It is clear that the bound pair is being reformed from the geminate partners at a rate that is at a maximum immediately after photolysis and slows progressively until it reaches a limiting value, which applies to a final exponential phase. In addition, the limiting exponential phase is temperature-dependent with an activation energy about 7 kcal mol^{-1}, but varies with the species of myoglobin (sperm whale or horse heart) and buffer conditions. Faster processes are much less temperature-dependent.

We measured the quantum yield for photodissociation, Q, using a procedure based on the method of Brunori and Giacometti (1981). The original method considers a general case, but when the photolysis pulse is only a few nanoseconds in duration, the situation simplifies. If we assume that, prior to a photolysis pulse all of the myoglobin proteins are liganded, Q may be defined as Q = (number of deliganded Mb existing after all geminate recombination is complete and before any subsequent bimolecular combination occurs)/(number of photons absorbed by Mb–X liganded Mb). If I is the irradiance incident on the sample, ϵ_p is the absorptivity at the photolysis (pump) wavelength, and the lowest order form of Beer's Law is assumed to apply, then within the irradiated volume,

$$\ln\left\{\frac{[\text{Mb–X}]_0}{[\text{Mb–X}]_t}\right\} = Q\epsilon_p I \tag{5}$$

The concentrations can be converted to absorbances using

$$\ln\left\{1 - \frac{\Delta A}{\Delta A_{max}}\right\} = Q\epsilon_p I \tag{6}$$

where ΔA is the absorbance change of the sample measured at the appropriate time, and ΔA_{max} is the absorbance change that would exist if all of the ligands could be dissociated. Although ΔA_{max} can be obtained from the published absorbance spectra of liganded and deliganded Mb, we also confirmed the value by preparing samples of deliganded Mb. Such samples are not very stable, but we believe that we achieved 10% precision. If we assume that the transient ΔA can be measured with sufficient accuracy, there remain three experimental problems that must be considered in order to avoid systematic error.

First, eq 6 is valid only for small irradiances. When I is large, there are additional considerations not included in the elementary theory, such as multiple photons being absorbed by the same protein or photoselection effects (Magde, 1978). Consequently, a reliable quantum yield determination requires measuring ΔA as a function of I and demonstrating a linear region at low I whose slope is proportional to Q.

Second, there must be a reliable means of determining I. The usual solution is to use a reference standard of known Q and carry out a relative, rather than absolute, determination. We used Mb–CO, which has a Q near unity; we assumed 0.95. Any small error there will make only a proportional percentage error in the Q for oxygen.

Third, one must ensure that all of the absorption at the pump wavelength and all of the changes at the probe wavelength are due to the intended process. Mb–O_2 is susceptible to degradation, both thermally and photolytically. We used a flowing sample cell with complete sample changes

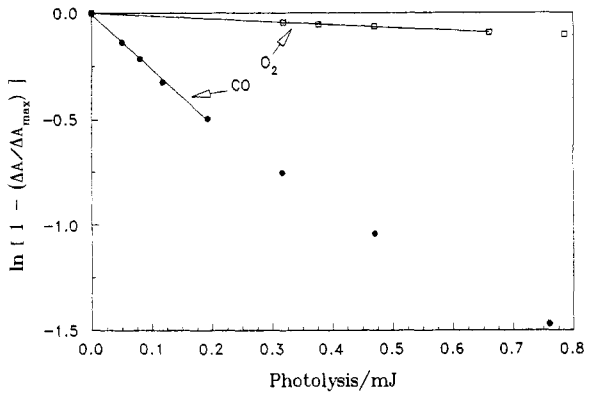

FIGURE 7: Limiting slope at low photolysis energy proportional to Q. The lines show the points considered. Slopes are −2.57 ± 0.06 for MbCO and −0.139 ± 0.003 for MbO_2. If Q(CO) is assumed to be 0.95, then $Q(O_2)$ = 0.057 ± 0.006.

between laser shots. The pump wavelength and the sample concentrations were selected so that the absorbed energy was identical for the Mb–O_2 sample and the Mb–CO reference.

Figure 7 shows the left-hand side of eq 6 plotted against the pump pulse energy for typical data runs on horse heart Mb–O_2 and Mb–CO in Bis-Tris buffer at pH 7.0. The probe wavelength was 437.5 nm, with a bandwidth of 2 mm. (Identical results were obtained at a bandwidth of 8 nm.) At that wavelength, the absorptivity for the probe is identical for the reference and the unknown. The pump wavelength was 540 nm. Note that the dependence on I becomes linear only at quite low pulse energies.

From these data, we determine Q = 0.057. Assignment of uncertainty based on one plot is not particularly useful, as the variation due to unknown factors from one day to another is more significant. Considering several experimental runs, we estimate the 90% confidence interval to be ±0.01.

Myoglobin–CO. Transient data for the picosecond photolysis of carboxymyoglobin from 0 to 50 ps were obtained at 13 and 37 °C. Singular values decreased steadily (at 13 °C: 11.0, 1.08, 0.35, 0.15, 0.11). Autocorrelation of V gives 0.92, 0.96, 0.88, 0.47, and 0.45. There is a rationale for considering the first three components to be significant, as determined by the autocorrelation values, but the overall trend is more suggestive of a spectrum that shifts as it decays. The results of SVD analysis of the Mb–CO data obtained at 37 °C are essentially identical.

Figure 8 shows the first three kinetic components from the SVD analysis of the Mb–CO data obtained at 13 °C, along with similar results for the data obtained at 37 °C. As with the myoglobin–oxygen data, the kinetic components are identical for the two temperatures. The first spectral component is that of a "deoxy minus oxy" Mb–CO species. Any detectable recombination is limited to very early times.

We fit the first kinetic component from the SVD analysis of the Mb–CO to a single exponential with a base-line offset in order to assess the effect of temperature. Both temperatures give τ = 6.0 ± 2 ps, k = (1.67 ± 0.5) × 10^{11} s^{-1}, and fractional decay = 14 ± 4%. The observed kinetics is the same within experimental error. A single exponential with offset is entirely adequate to fit the decaying portion of kin1. Again, these experiments show that the rate and amount of geminate recombination of ground-state Mb–CO, if any, between 0 and 50 ps are not temperature-dependent near room temperature. If the decay is due to spectral relaxation, then that process is not temperature-dependent.

Myoglobin–NO. Transient data were acquired between 0 and 750 ps at 15 and 32 °C. At 15 °C, the autocorrelation

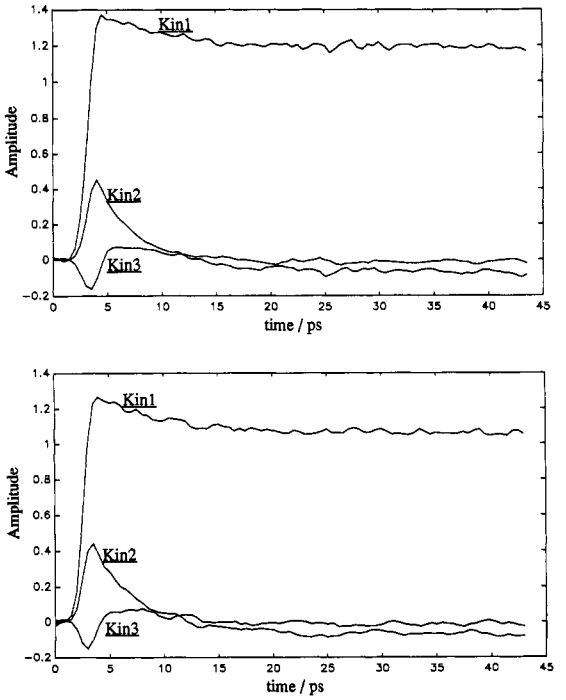

FIGURE 8: First three kinetic components obtained from the SVD analysis of the MbCO data obtained at 13 (top) and 37 °C (bottom).

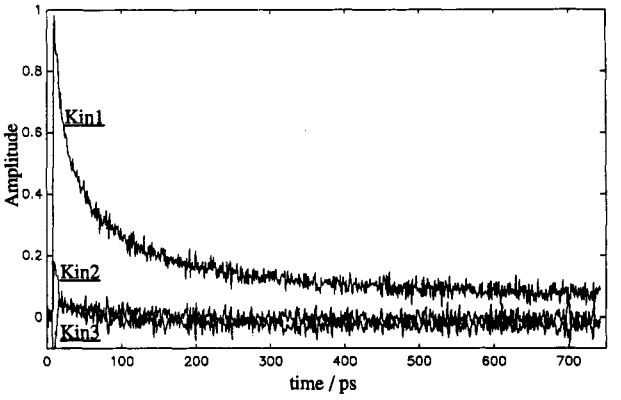

FIGURE 9: First three kinetic components obtained from the SVD analysis of the MbNO data obtained at 15 °C.

of V is 0.983, 0.787, 0.691, 0.466, and −0.108, and the singular values are 5.58, 0.87, 0.74, 0.58, and 0.45. The results are similar to those obtained for Mb–O_2 and Mb–CO. As with the other ligands, the third and later components may be distorted by limited precision in the correction for the temporal dispersion in the probe beam. It is unlikely that there are multiple distinct intermediates. There may well be a spectral shift associated with a decaying transient. The SVD results for the Mb–NO data at 32 °C are similar to those at 15 °C.

Figure 9 shows the first three kinetic components for the SVD analysis of the Mb–NO data set at 15 °C. They show the same patterns that were observed for the Mb–O_2 and Mb–CO data. The spectral component that corresponds to the first kinetic component is a "deoxy minus oxy" spectrum. The spectral component that corresponds to the second kinetic component shows a red edge and is similar to those observed for the other ligands. However, the first kinetic component for the Mb–NO data is very different from the first kinetic components obtained for the other ligands in that it is clearly not a single-exponential decay, even on this limited time scale.

We attempted to fit double exponentials to the decay of kin1 by fitting 200, 400, 600, or 750 ps of the decay. The

Table 3: Fits to the SVD Analysis of Mb–NO

sample (temp, °C)	length of fit	fast component		slow component		base-line offset amplitude
		amplitude	lifetime (ps)	amplitude	lifetime (ps)	
Mb–NO (15)	200	0.39	9.5	0.48	69	0.14
Mb–NO (32)	200	0.31	6.5	0.52	60	0.17
Mb–NO (15)	400	0.45	12	0.43	95	0.11
Mb–NO (32)	400	0.41	12	0.44	99	0.12
Mb–NO (15)	600	0.49	15	0.39	120	0.09
Mb–NO (32)	600	0.46	16	0.39	132	0.09
Mb–NO (15)	750	0.52	16	0.36	134	0.08
Mb–NO (32)	750	0.49	19	0.36	150	0.08

results from this are given in Table 3 for the data collected at 15 and 32 °C. For this purpose, the kinetic components were scaled to the sample amplitude in order that comparisons might be more easily made. This a commonly used test to determine whether a decay is a true double exponential. Table 3 shows that, as longer and longer portions of the data are fit, the lifetimes for the fast and slow components continually increase. This indicates that the decay is not a double exponential.

As with the other ligands, for Mb–NO there is little variation either in the geminate recombination rate or in the amount of geminate recombination as a function of temperature near room temperature.

DISCUSSION

Methods. Petrich and co-workers (1991) argue that the older multichannel detector technology based on vidicons is inadequate for precise kinetic studies, citing our earlier study (Jongeward et al., 1988) as an example. We agree. Although many of the shortcomings of vidicon-based measurements were due to the fact that the delay line was adjusted manually, those manual methods persisted because mediocre vidicon performance did not justify improving other aspects of the procedure. Petrich and co-workers (1991) suggest that better results are obtained with photodiode detectors. Again we agree, but we suggest that, if one diode is good, several hundred are even better.

Multiwavelength detection using diode arrays or charge-coupled devices should be much superior to single-wavelength detection. If care is taken in synchronizing readout with laser firing and delay line movement, the diode array gives noise performance comparable to that of single diodes. The major source of scatter in measurements reported here is fluctuation in the laser pulse energy, combined with finite data acquisition times, which are limited by sample lifetime. The latter limitation implies that translating, spinning, or flowing samples must be used.

Multiwavelength analysis is always an advantage, but we believe that in the low-picosecond time range it is essential. In that regime, we cannot assume that we know the characteristics of chemical intermediates. We must assume that any species produced will not exist in thermal equilibrium, but will be electronically and vibrationally excited. For large polymeric species, such as proteins, such nonequilibrium behavior may persist to much longer times. Kinetic analyses undertaken at selected single wavelengths may, of course, be correct by chance. Their inadequacy comes not in measuring the rate constants but in confirming that the basic model is correct. Multiwavelength analysis, however, poses a problem. How should one analyze a data set consisting of a million absorbance values? Global analysis by SVD has the outstanding advantage that it provides a mathematically robust solution to selecting the most salient features, ranking smaller components in order of importance and reducing random noise. It eliminates investigator bias in selecting the "most appropriate" wavelength for analysis. We were driven to SVD when we found that by minor changes we could produce a variety of different "results". However, it is important to note that SVD is not magic. It generates, from an unwieldy set of absorbance values, a manageable set of a few spectra and a few kinetic traces. At that point, there is as much room for interpretation as ever. The spectra generally do not correspond to any particular chemical species. We may expect that with further experience protocols will emerge for the best ways to take advantage of SVD analyses. In this report, we offer some simple interpretations for SVD components at early picosecond times, where multiple components evolve rapidly. However, the main point of our SVD treatment is not that we have solved the very difficult spectral identifications in that regime—we have not. The important thing to stress occurs in the opposite time regime. Over many decades of time after 10 ps, there is one dominant transient spectrum according to rigorous SVD analysis.

Quantum Yields for Photodissociation. We assume that the mechanism for photodissociation of a ligand in myoglobin may be written as

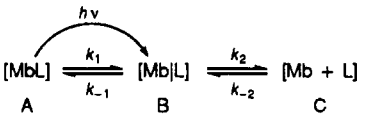

(7)

where A represents the ligand bound to the iron in the heme structure in the protein, B is the geminate pair with the iron–ligand bond broken but the ligand still within the protein, and C represents deliganded Mb alone with solvated free ligand. Questions arise as to whether the species B formed by photolysis is the same as any species present along the pathway of thermal reactions, whether B is a single species, a small number of distinguishable species, or a continuum, and so on, but there is no longer any question that something like B exists for hundereds of nanoseconds after photolysis.

One basic parameter characterizing this model is the quantum yield for photodissociation, Q, defined as the number of moles of C produced for each einstein of photons absorbed by A, in the limit of low light intensity. Although there seem to be no detailed descriptions of very precise measurements, it is accepted that Q is independent of the excitation wavelength over a broad range of visible and ultraviolet wavelengths. Long before time-resolved studies of B were possible, it was already known that Q varied widely for different ligands (Antonini & Brunori, 1971). For carbon monoxide, Q is very close to unity. It may vary with conditions, but for Mb in typical buffers at any temperature near ambient, it is unlikely to be much below 90%. Nitric oxide represents the opposite extreme, with Q as low as 0.1%. We know from our own efforts that $Q(NO)$ is at least a factor of 10 lower than $Q(O_2)$. As an

intermediate case, oxygen is particularly important. We were confused for a time by discordant reported values. The early number (Antonini & Brunori, 1971) was 5%. A later report (Gibson et al., 1986) suggested 13%, which was significantly higher and more appealing to us in interpreting our first picosecond data on oxymyoglobin (Jongeward et al., 1988). Another recent report seems to favor the lower number, but it is concerned primarily with low temperatures and does not claim to offer a precision determination at room temperature (Chance et al., 1990). Consequently, we made a careful remeasurement and found $Q(O_2) = 5.7 \pm 1\%$, in support of the smaller value.

By themselves, quantum yields for dissociation are not easy to interpret. Small Q's might imply low probability that B is formed from A following absorption of a photon, or it might imply that the back-reaction from B to A competes effectively with the ligand escape from the protein that is required to form C from B. However, the known values for Q represent essential boundary conditions that must be satisfied by any interpretation of transient spectra, a point compellingly made by Gibson and co-workers (1986).

Nanosecond Kinetics. For MbCO, there is a prominent photolysis signal due to ligand dissociation and very little recombination of the geminate pair. Some years ago, Henry and co-workers (1983) reported 4% geminate recombination with an observed lifetime of 180 ns, implying a bond formation rate constant near 2×10^5 s^{-1}. This also demonstrates that CO remains in the protein for about as long as O_2, which we expect since they are similar in size and polarity. In Hb, where there is more geminate recombination, it is quite clear that CO is trapped in the protein for such times (Campbell et al., 1985).

Geminate recombination in MbO_2 is exponential at long times (>100 ns) in liquid solutions at ambient temperatures. It is significant that the asymptotic behavior is strictly exponential. This means that, at least at long times, the kinetic description of eq 7 is appropriate. There is some gatelike mechanism that controls escape from the protein. The ligand "attempts" many times to pass the "gate" and succeeds randomly with a probability that is constant over this time regime. Rebinding to the iron has the same properties: many attempts, random success, and a rate constant independent of time for times longer than a few tens of nanoseconds. There could be (and no doubt are) multiple conformations for the geminate pair, but equilibrium among them is reached by this time for liquid solutions at ambient temperature. Other descriptions of geminate recombination have been proposed that imply nonexponential asymptotic behavior even at ambient conditions, but they are now ruled out by experiment. The fact that there is an activation energy for k_2 and k_{-1} in the nanosecond process (Chatfield et al., 1990) provides additional justification for the kinetic description.

Although the asymptotic exponential behavior is well-substantiated, the same rate constants do not apply at early times. As soon as digital recording and signal averaging replaced single-shot oscilloscope traces, we had an indication that the kinetic trace was "steeper" at early times (Campbell, 1985). One must, however, take pains to exclude electronic artifacts. Eventually, we were able to convince ourselves that the geminate recombination in MbO_2 is nonexponential, displaying additional faster components at early time. We could barely detect them at room temperature, but they became clear at slightly lower temperatures (Chatfield et al., 1990). The details depend on both buffer conditions and the species of Mb. As far as we could extrapolate from nanosecond recordings, k_{obs} is larger at early nanosecond times by a factor of about 10, compared to the limiting value at longer times. We showed that one might concoct mechanisms involving two intermediates that reproduce those biexponential kinetics, but it was not easy to do so and the assignments were not compelling. Other work has explored environmental effects on biexponential nanosecond kinetics (Sato et al., 1992).

Our objective here is to demonstrate that the rate of geminate recombination continuously changes (slows) over time before reaching the asymptotic exponential limit. In MbO_2, we not only knew that recombination is multiexponential after 20 ns, but once $Q(O_2)$ was confirmed to be 0.057, we knew that there should be additional, faster geminate recombination at earlier times. At 20 ns there is less than twice the amount of dissociation that is present at long times. In other words, if $Q(O_2)$ is 0.057, then about 8–10% (depending on temperature) of the ligands is dissociated at 20 ns. Either the other 90% of the Fe–O_2 bonds is never broken or there is faster geminate recombination. Those earlier times are considered in the section on picosecond geminate recombination.

For MbNO, nanosecond recombination is not observed because picosecond recombination is so efficient. No photolysis signal is observed at times longer than 10 ms under conditions where each protein adsorbs only one photon per "shot". This is consistent with the low Q(NO), but yields no kinetic information.

Picosecond Geminate Recombination. It is our hypothesis that, immediately after photolysis, recombination of geminate partners occurs at rates much faster than those suggested by the asymptotic values that characterize recombination over hundereds of nanoseconds. Either multiple rate constants must be assigned to a sequence of different forms of geminate pairs or the recombination must be described with a time-changing rate constant that decreases monotonically and continuously.

The least satisfying arguments applies to MbCO, but what data there are support the hypothesis. Since at least 90% and possibly 95% of all photodissociated CO escapes from Mb, it is difficult to measure any recombination, left alone decipher changing rates. The only explicit statement about CO picosecond geminate recombination in Mb is that by Anfinrud and co-workers (1989), based on time-resolved infrared absorption. Since the vibrational stretching frequency is significantly different for bound and unbound CO, they could detect a rapid appearance of free CO after photolysis, followed by a slight (5%) diminution of the transient signal over 1 ns and no detectable further change at longer times. This implies a rate constant for bond formation, k_{-1}, near 10^8 s^{-1}. Such a rate cannot persist much beyond a nanosecond; it must evolve to a smaller value. As discussed above, Henry et al. (1983) report observing small amounts of nanosecond recombination, from which one could infer $k_{-1} \approx 10^5$ s^{-1} at long times. Although this line of reasoning is attractive, it must be conceded that both experiments are very difficult, and there is litle hope of further refinement to decide whether there are two distinct kinetic intermediates or a continuously evolving recombination rate. Our own measurements in the visible region were unable to add anything to the argument. Time-resolved IR has also been applied to Mb by another group (Rothberg, 1990).

The major feature of the transient visible spectrum occurs at earlier times, namely, a rapid change in the first few picoseconds. The transient IR study (Anfinrud et al., 1989) did not find evidence for ultrafast recombination of the free CO on that time scale. Computer simulations (Straub & Karplus, 1991) concur with the experimental finding that all

released CO is formed in its vibrational ground state and is rotationally and translationally equilibrated in less than 10 ps. It is also the case that 5-coordinate Mb, already without a ligand, exhibits a somewhat similar transient after photoexcitation. The SVD analysis proves conclusively that these rapid changes cannot be interpreted by postulating just two unchanging species, because the second and probably third eigenvectors are significant. We interpret total SVD analysis to demonstrate that, at early times, there is a continually shifting spectrum due mainly to relaxation (cooling) of the newly formed 5-coordinate heme, as predicted by molecular dynamics simulations by Henry et al. (1986). Time-resolved Raman studies are also consistent with this interpretation and agree that the time scale is a few picoseconds (Alden et al., 1990; Lingle et al., 1991), although there is some controversey (Li et al., 1992). Similar transient visible absorption spectra have been observed and analyzed in other porphyrins (Rodriguez et al., 1991). There may be some recombination of CO with unrelaxed heme, but it is certainly less than 10%. The transient IR results seem to require that any primary geminate recombination be accomplished in less than a picosecond. (Of course, a small amount of CO could recombine while a comparable amount of hot CO cooled, giving no net change in the transient IR spectrum, but that would be coincidental.) It would not be surprising if any primary geminate recombination were extremely fast, considerably below a picosecond.

Evidence is growing that the "intimate pair" recombination in small, simple molecules occurs after a single collision or not at all (Schwartz et al., 1993). A few percent femtosecond recombination permits a simple interpretation of the complex shifting transient absorption spectra: red-shifted "hot band" absorption of the deliganded Mb cools and its absorption shifts from about 470 to 440 nm, while "hot band" absorption of any recombined MbCO shifts from about 450 to 420 nm. However, the situation could be more complicated with excited electronic states also present. It is valuable, regardless, to have this CO result, because it reveals what the signal due to (almost) 100% dissociated heme looks like. There is no variation with temperature of the fast signals that we could determine.

Oxygen is the most important ligand, yet it has been studied the least. We explained above that the asymptotic value of bond formation, k_{-1}, does not apply at earlier times. There is a temperature-dependent faster recombination evident on the 20–50-ns time scale. In addition, there is a faster recombination observable over the 2–10-ns time scale, where k_{-1} appears to be about 1.3×10^8 s^{-1}. Still, this does not account for the small $Q(O_2)$. At 1 ns the amount of 5-coordinate iron is only about 4–6 times as large as it is on the millisecond time scale. Since $Q(O_2) = 5.7\%$, only 25–35% of the ligands is dissociated at 1 ns. There may be a small amount of excess recombination over the time 0.1–1 ns taking place with yet higher k_{-1}, but k_{-1} cannot be as large as 10^9 there or we would have seen larger effects than we did. All of this implies that about 60–70% of the oxygen never dissociates or that it recombines in the first few picoseconds, with a rebinding rate k_{-1} in excess of 10^{11} s^{-1} The SVD analysis demonstrates a large decay of kin1 at this rate. However, the amplitude change is still too small at slightly less than 50%, and the spectral components resolved and the time evolution do not differ much from those recorded for CO dissociation. The likely interpretation is that much, if not all, of the fast recombination takes place at subpicosecond times and that the rate-limiting process observed is thermalization. Some recombination may take place over the few picosecond interval, but the partners are not completely thermalized and the rate constants are not necessarily applicable to relaxed species. In any case, there is either very fast bond formation or bonds are not broken in the first place.

There is no variation with temperature of the picosecond processes. This is not surprising if they involve species that are already "hot". In contrast, the nanosecond processes do vary with temperature. This applies not only to the observed rates but also to both k_{-1} and k_2 separately. After some nanoseconds, rebinding requires a certain amount of conformational change in the protein, and escape of the ligand from the protein really does involve something like a gate that "swings open" by thermal activation. The fastest recombination in MbO_2 that certainly involves ground-state partners (measured over the 1–10-ns time scale) remains somewhat uncertain in its temperature dependence. We did not observe any change with temperature, which tends to suggest that the activation needed is less than that at longer times, but the precision is not sufficient to be any more definite.

Nitric oxide is the easiest ligand to discuss, since recombination is nearly complete over a time range that is easy to measure using time-of-flight picosecond methods. The earliest time behavior is not very different from that of dioxygen. The SVD analysis shows quite similar basis spectra and kinetic components, implying rather similar vibrational relaxation. The amplitude of the transient at zero time delay is similar in all three ligands, suggesting that the assumption of 100% dissociation is reasonable. If so, there must be either subpicosecond recombination followed by vibrational cooling or recombination taking place simultaneously with a thermalization process. The distinction is not essential to our argument. What is clear is that recombination of the thermalized pairs follows smoothly after the early picosecond processes. It continues with a progressively slower rate that cannot be fit well with two exponentials. Furthermore, we argue that the rate must decrease further. The slowest rate we deduce from curve fitting is 7×10^9 s^{-1}. We again assume that NO must remain in the protein for more than 100 ns. If this rate persisted, $Q(NO)$ would be less than 10^{-4}, which is even lower than the value of 10^{-3} that is customarily quoted (Antonini & Brunori, 1971).

We find no variation of geminate recombination in NO as the temperature is changed. This is very significant. It means that not only do the very fast processes, which involve nonthermalized species, have no activation energy but even the recombination of ground-state partners has little or no activation energy until some protein relaxation occurs over nanosecond times.

The experimental results for NO are very similar to those reported by Petrich et al. (1991). Our interpretations are broadly similar too. We note two differences: we used SVD, which we believe gives more credence to the results, and we examined the temperature variation of recombination, an important part of any kinetic study. It is gratifying to be able to document picosecond studies that agree in some detail.

A number of studies have monitored aspects of protein kinetics and been interpreted as evidence of conformational change, either in gross structure or in details of the heme prosthetic group. A sampling was cited in the introduction that is sufficient to suggest that protein conformation relaxes on all time scales. Although such changes should affect the rebinding rate constant in a continuously evolving manner, the effects are only evident experimentally in regions where the rate constant has a suitable value. For Mb combining

with different ligands that falls in different time regimes: picoseconds for NO, early nanoseconds for O_2, and not at all for CO.

We have only occasionally referred to hemoglobin geminate recombination with ligands in the above analysis. Hemoglobin is a more complicated protein, and we believe that it is essential to understand myoglobin independently, without being swayed by a possibly defective analogy. However, once we are persuaded that we understand Mb, the analogous behavior in Hb is striking (Friedman et al., 1985). The emphasis at that time was somewhat different, and some inferences were more tentative than they might be today, but with the benefit of today's perspective the nonexponential decay curves recorded between 0.1 and 2.4 ns are understandable. Furthermore, in Hb there is considerable recombination with CO. We have confirmed (unpublished) Friedman's observation that CO in Hb shows a decreasing recombination rate in the early nanosecond time scales, just as O_2 does in Mb.

CONCLUSION

After the photodissociation of liganded myoglobin, the ligand remains in the protein for several hundered nanoseconds, on average. The geminate partners recombine with kinetics that are not single exponential. For the diatomic ligands O_2 and NO, and quite likely CO as well, the experimental geminate recombination data are not fit well even by two or three exponentials. Since other lines of argument also point to protein conformational changes following photolysis, we believe that there is adequate justification now to invoke something like the Agmon–Hopfield hypothesis of a continuously evolving recombination rate. (There could also be an evolving probability for ligand escape as the protein relaxes.)

We add, however, that many mechanisms may be consistent with any set of kinetic data. Molecular dynamics simulations of ligand diffusion, even in a rigid protein, can give behavior like that observed for NO, that is, nonexponential rebinding over 100 ps (Elber, 1993). Whether a broad heterogeneous distribution of reaction partners narrows as fast-reacting forms react or a narrow distribution exists in an evolving environment is not addressed by our experimental results. Our more limited goal is to establish that the observed recombination rate evolves more or less continuously over time. Furthermore, at early time, recombination rates are independent of temperature; there is little or no activation energy. On the nanosecond time scales, rates become dependent on temperature, and at that time an activation barrier has become established.

Much of our data echoes some previous results, while diverging from others. The conclusion should be reliable because it involves an integrated study of all ligands at all time scales and includes temperature effects. The data are also noteworthy as the first global analysis of time-resolved picosecond absorption using singular value decomposition. The SVD treatment proves that, after the first few picoseconds, we have a single kinetic relaxation dominating, despite the nonexponential behavior. Conversely, SVD shows that, within the first few picoseconds, we must have either several distinct components or, more likely, continuously shifting spectral components. On the basis of similarities in the shape of spectral and kinetic components, but differences in amplitudes, we prefer a model in which dissociation is 100% in all cases, but primary geminate recombination varies. This primary recombination may well be very fast (subpicosecond). The rate of spectral relaxation probably has little to do with the rate of primary geminate recombination itself other processes being rate-limiting. Our eq 1 or 7 with conventional rate constants is not appropriate for the intimate pair, which never exists in a thermally equilibrated form. Nevertheless, varying amounts of primary geminate recombination take place for the different ligands, as revealed by different amplitudes in the early picosecond relaxation.

Large ligands exhibit somewhat different behavior, as we showed previously, with much less evidence for continuously evolving rate constants (Jongeward et al., 1988). We found it remarkable in these early studies that isocyanides seemed to have kinetics similar to oxygen, despite having spin properties like CO. Now that O_2 is better characterized, the similarity to isocyanides is less pronounced. The isocyanides may be more like CO, but are prevented by steric considerations from moving away from the iron and, consequently, show enhanced recombination probability.

Once a continuously evolving rate is accepted for geminate recombination, the question still remains of whether control is due primarily to the proximal or distal effects. These may be distinguished in proteins that are modified by site-selective mutations. They can also be addressed in biomimetic model compounds. We reported the beginnings of such a distinction (Traylor et al., 1990) and are continuing with new models that better mimic the sort of behavior we observe in myoglobin.

ACKNOWLEDGMENT

We appreciate the interest and help of Tammy M. Grogan and Prof. T. G. Traylor.

REFERENCES

Agmon, N., & Hopfield, J. J. (1983) *J. Chem. Phys. 79*, 2042–2053.

Agmon, N., & Rabinovich, S. (1992) *J. Chem. Phys. 97*, 7270–7286.

Alberding, N., Chan, S. S., Eisenstein, L., Frauenfelder, H., Good, D., Gunsalus, I. C., Nordland, T. M., Perutz, M. F., Reynolds, A. H., & Sorenson, L. B. (1978) *Biochemistry 17*, 43–51.

Alden, R. G., Chavez, M. D., Ondrias, M. R., Courtney, S. M., & Friedman, J. M. (1990) *J. Am. Chem. Soc. 112*, 3241–3242.

Alpert, B., El Mohshni, S., Linqvist, L., & Tfibel, F. (1979) *Chem. Phys. Lett. 64*, 11–16.

Anfinrud, P. A., Han, C., & Hochstrasser, R. M. (1989) *Proc. Natl. Acad. Sci. U.S.A. 86*, 8387–8391.

Ansari, A., DiIorio, E. E., Dlott, D. D., Frauenfelder, H., Iben, I. E. T., Langer, P., Roder, H., Sauke, T. B., & Shyamsunder, E. (1986) *Biochemistry 25*, 3139–3146.

Ansari, A., Berendzen, J., Braunstein, D., Cowen, B. R., Frauenfelder, H., Hong, M. K., Iben, I. E. T., Johnson, J. B., Ormos, P., Sauke, T. B., Scholl, R., Schulte, A., Steinbach, P. J., Vittitow, J., & Young, R. D. (1987) *Biophys. Chem. 26*, 337–355.

Antonini, E., & Brunori, M. (1971) in *Hemoglobin and Myoglobin in Their Reactions with Ligands*, Vol. 21, North-Holland, Amsterdam.

Austin, R. H., Beeson, K. W., Eisenstein, L., Frauenfelder, H., & Gunsalus, I. C. (1975) *Biochemistry 14*, 5355–5373.

Beece, P., Eisenstein, L., Frauenfelder, H., Good, D., Marden, M. C., Reinisch, L., Reynolds, A. H., Sorensen, L. B., & Yue, K. T. (1980) *Biochemistry 19*, 5147–5157.

Berlin, Y. A., Chekunaev, N. I., & Goldanskii, V. I. (1992) *Chem. Phys. Lett. 197*, 81–85.

Bizzori, A. R., & Cannistraro, S. (1992) *Biophys. Chem. 42*, 79–85.

Brunori, M., & Giacometti, G. M. (1981) *Methods Enzymol. 76*, 582–595.

Campbell, B. (1985) Ph.D. Thesis, University of California at San Diego, La Jolla, CA.

Campbell, B. F., Magde, D., & Sharma, V. S. (1985) *J. Biol. Chem. 260*, 2752–2756.
Champion, P. M. (1992) *J. Raman Spectrosc. 23*, 557–567.
Chance, M. R., Courtney, S. H., Chavez, M. D., Ondrias, M. R., & Friedman, J. M. (1990) *Biochemistry 29*, 5537–5545.
Chatfield, M. D., Walda, K. N., & Magde, D. (1990) *J. Am. Chem. Soc. 112*, 4680–4687.
Dasgupta, S., Spiro, T. G., Johnson, C. K., Dalickas, G. A., & Hochstrasser, R. M. (1985) *Biochemistry 24*, 5295–5297.
Duddell, D. A., Morris, R. J., & Richards, J. T. (1979) *J. Chem. Soc., Chem. Commun.* 75–76.
Elber, R. (1993) Reported at the Sixth International Conference on Bioinorganic Chemistry, La Jolla, CA.
Elber, R., & Karplus, M. (1987) *Science 235*, 318–321.
Findsen, E. W., Friedman, J. M., Ondrias, M. R., & Simon, S. R. (1985) *Science 229*, 661–665.
Friedman, J. M., Scott, T. W., Fisanick, G. J., Simon, S. R., Findsen, E. W., Ondrias, M. R., & MacDonald, V. W. (1985) *Science 229*, 187–190.
Genberg, L., Heisel, F., McLendon, G., & Miller, R. J. D. (1987) *J. Phys. Chem. 91*, 5521–5524.
Gibson, Q. H., Olson, J. S., McKinnie, R. E., & Rohlfs, R. J. (1986) *J. Biol. Chem. 261*, 10228–10239.
Greene, B. I., Hochstrasser, R. M., Weisman, R. B., & Eaton, W. A. (1978) *Proc. Natl. Acad. Sci. U.S.A. 75*, 5255–5259.
Henry, E. R., Sommer, J. M., Hofrichter, J., & Eaton, W. A. (1983) *J. Mol. Biol. 166*, 443–451.
Henry, E. R., Eaton, W. A., & Hochstrasser, R. H. (1986) *Proc. Natl. Acad. Sci. U.S.A. 83*, 8982–8986.
Hofrichter, J., Henry, E. R., Sommer, J. H., Deutsch, R., Ikeda-Saito, M., Yonetani, T., & Eaton, W. A. (1985) *Biochemistry 24*, 2667–2679.
Jongeward, K. A., Magde, D., Taube, D. J., Marsters, J. C., Traylor, T. G., & Sharma, V. S. (1988) *J. Am. Chem. Soc. 110*, 380–387.
Lambright, D. G., Balasubramanian, S., & Boxer, S. G. (1991) *Chem. Phys. 158*, 249–260.
Li, P., Sage, J. T., & Champion, P. M. (1992) *J. Chem. Phys. 97*, 3214–3227.
Lingle, R., Jr., Xu, X., Zhu, H., Yu, S. C., & Hopkins, J. B. (1991) *J. Phys. Chem. 95*, 9320–9331.
Magde, D. (1978) *J. Chem. Phys. 68*, 3717–3733.
Martin, J. L., Migus, A., Poyart, C., Lecarpentier, Y., Astier, R., & Antonetti, A. (1983) *EMBO J. 2*, 1815–1819.
Murray, L. P., Hofrichter, J., Henry, E. R., & Eaton, W. A. (1988) *Biophys. Chem. 29*, 63–76.
Nöe, L. J., Eisert, W. G., & Rentzepis, P. M. (1978) *Proc. Natl. Acad. Sci. U.S.A. 75*, 593–577.
Petrich, J. W., & Martin, J. L. (1989) *Chem. Phys. 131*, 31–47.
Petrich, J. W., Poyart, C., & Martin, J. L. (1988) *Biochemistry 27*, 4049–4066.
Petrich, J. W., Lambry, J. C., Kuczera, K., Karplus, M., Poyart, C., & Martin, J. L. (1991) *Biochemistry 30*, 3975–3987.
Rodriguez, J., Kirmaier, C., & Holten, D. (1991) *J. Chem. Phys. 94*, 6020–6028.
Rothberg, L., Jedju, T. M., & Austin, R. H. (1990) *Biophys. J. 57*, 369–373.
Sato, F., Sakaguchi, Y., Hayashi, H., Iizuka, T., & Shiro, Y. (1992) *Biochem. Biophys. Acta 1122*, 299–304.
Schneebeck, M. C., Vigil, L. E., Friedman, J. M., Chavez, M. D., & Ondrias, M. R. (1993) *Biochemistry 33*, 1318–1323.
Schwartz, B. J., King, J. C., Zhang, J. Z., & Harris, C. B. (1993) *Chem. Phys. Lett. 203*, 503–508.
Scott, T. W., & Friedman, J. M. (1984) *J. Am. Chem. Soc. 106*, 5677–5687.
Sommer, J. H., Henry, E. R., & Hofrichter, J. (1986) *Biochemistry 24*, 7380–7388.
Steinbach, P. J., Loncharich, R. J., & Brooks, B. R. (1991) *Chem. Phys. 158*, 383–394.
Straub, J. E., & Karplus, M. (1991) *Chem. Phys. 158*, 221–248.
Tian, W. D., Sage, J. T., Šrajer, V., & Champion, P. M. (1992) *Phys. Rev. Lett. 68*, 408–411.
Traylor, T. G., Taube, D. J., Jongeward, K. A., & Magde, D. (1990) *J. Am. Chem. Soc. 112*, 6877–6880.
Xie, X., & Simon, J. D. (1990) *J. Am. Chem. Soc. 112*, 7802–7803.
Young, R. D., Frauenfelder, H., Johnson, J. B., Lamb, D. C., Nienhaus, G. U., Philipp, R., & Scholl, R. (1991) *Chem. Phys. 158*, 315–327.